Journal of Chromatography B 1099 (2018) 56–63

Contents lists available at ScienceDirect

Journal of Chromatography B

journal homepage: www.elsevier.com/locate/jchromb

Analysis of lipoprotein-specific lipids in patients with acute coronary syndrome by asymmetrical flow field-flow fractionation and nanoflow liquid chromatography-tandem mass spectrometry

Jae Hyun Lee[a], Joon Seon Yang[a], Sang-Hak Lee[b,c,*], Myeong Hee Moon[a,*]

[a] Department of Chemistry, Yonsei University, Seoul 03722, Republic of Korea
[b] Division of Cardiology, Department of Internal Medicine, Severance Hospital, Yonsei University College of Medicine, Seoul 03722, Republic of Korea
[c] Cardiovascular Research Institute, Yonsei University College of Medicine, Seoul 03722, Republic of Korea

ARTICLE INFO

Keywords:
Acute coronary syndrome
Coronary artery disease
Lipidomic analysis
Lipoprotein
nUPLC-ESI-MS/MS
Flow field-flow fractionation

ABSTRACT

A comprehensive lipid analysis was performed at the plasma lipoprotein level in patients with acute coronary syndrome (ACS) and stable coronary artery disease (CAD). Because the lipids in lipoproteins are related to the pathology of the cardiovascular system, lipoprotein-specific lipid analysis can be useful for understanding the mechanism of lipid-associated cardiovascular diseases. Lipoproteins were size-sorted into high density lipoproteins (HDL) and low density lipoproteins (LDL) using asymmetrical flow field-flow fractionation, then lipids of each lipoprotein were analysed using nanoflow ultrahigh performance liquid chromatography-electrospray ionization-tandem mass spectrometry. A total of 365 lipids were structurally identified and quantified by selected reaction monitoring method. Two high abundance lysophosphatidylcholines (16:0 and 18:0) were significantly increased only in the HDL of the ACS group (vs. the stable CAD group). Phosphatidylethanolamines (38:5 and 40:5) significantly increased in ACS by > 2-fold in both lipoproteins. (18:0, 22:6)-diacylglycerol increased in ACS by 3.5-fold only in LDL; however, most high abundance triacylglycerols decreased 2-fold in both lipoproteins. The present study revealed the usefulness of lipoprotein-specific analysis of lipids in distinguishing ACS from stable CAD, and the selected lipids analysed in this study may be useful in the development of lipid markers for the early detection of ACS.

1. Introduction

Coronary artery disease (CAD) is the most common form of heart disease and is caused by the accumulation of atherosclerotic plaque in the arterial wall [1]. In addition, acute coronary syndrome (ACS) includes unstable angina, myocardial infarction, and sudden cardiac death which can occur in the course of CAD when atherosclerotic plaques suddenly rupture within coronary arteries, leading to a decreased blood flow. Pathophysiology of ACS was known to be affected by factors including thrombosis-related molecules [2]. However, determinants of ACS have not been completely elucidated and still under investigation.

Lipoproteins are globular complexes containing proteins and lipids in the blood system, and they transport fats and cholesterols to the body. Because lipids play several roles including cell signaling, energy storage, and forming cellular structures, their abnormal metabolism has been reported to be linked with several metabolic diseases such as diabetes, obesity, and atherosclerosis [3,4]. Molecular lipid species with diverse biological functions have been associated with the physiology and pathology of the cardiovascular system. To date, a broad range of lipid classes, including phosphatidylcholine (PC), lysophosphatidylcholine (LPC), ceramide (Cer), and cholesteryl ester, have been linked to cardiovascular disease or recognized as risk factors for cardiovascular disease [5–7]. The levels of a few lipid species change after pharmacologic therapy [8] and these are considered potentially useful for clinical monitoring [9].

Most studies of unbiased high throughput lipid analysis, or lipidomics, have used entire blood samples as sources of metabolites [10]. Therefore, the characteristics or clinical implications of the overall or specific pattern of lipids found in each lipoprotein have not been completely determined. A few studies evaluated the differential characteristics of lipids found in specific lipoproteins according to their classes [11] or individual health conditions [12]. Recently, the profiling of oxidized phospholipids in different lipoproteins from patients plasma

* Corresponding authors.
E-mail addresses: shl1106@yuhs.ac (S.-H. Lee), mhmoon@yonsei.ac.kr (M.H. Moon).

https://doi.org/10.1016/j.jchromb.2018.09.016
Received 27 July 2018; Received in revised form 7 September 2018; Accepted 13 September 2018
Available online 14 September 2018
1570-0232/

with CAD was determined using flow field-flow fractionation to sort the lipoproteins by size into high density lipoprotein (HDL) and low density lipoprotein (LDL), and oxidized phospholipids from each lipoprotein fraction of CAD patients were analysed in comparison to healthy controls by nanoflow liquid chromatography-electrospray ionization-tandem mass spectrometry (nLC-ESI-MS/MS) [13]. A feasibility study of a dual extraction strategy for the simultaneous analysis of lipids and proteins in lipoproteins used sequential density gradient ultracentrifugation to fractionate HDL and LDL in human and mouse plasma samples [14]. Because the development of CAD is closely associated with LDL oxidation [15,16], a comprehensive analysis of lipid profiles according to the type of lipoproteins can be useful to differentiate the pathogenesis of ACS from stable CAD. However, the lipidomic profiles at the lipoprotein level in those with ACS have not yet been examined.

In this study, a comprehensive lipidomic analysis was performed with different lipoproteins from patients with ACS and compared to those from patients with stable CAD. Plasma lipoproteins were size-sorted into HDL and LDL using semi-preparative scale asymmetrical flow field-flow fractionation (AF4). AF4 is an elution-based separation technique that can sort biological macromolecules, such as proteins, DNA, exosomes, organelles, and cells, by size in an open channel space [17–21] and it provides narrow size fractions of intact sample components that are suitable for further analysis with mass spectrometry or other biological methods [20–23]. Lipids in each lipoprotein fraction were analysed to identify the untargeted lipid molecular structures first and were quantified using high speed nanoflow ultrahigh performance LC-ESI-MS/MS (nUPLC-ESI-MS/MS) with the selected reaction monitoring (SRM) method. Finally, changes in lipoprotein-specific lipid profiles of patients with ACS were compared to those of patients with stable CAD.

2. Materials & methods

2.1. Chemicals and reagents

A total of 32 lipid standards were purchased from Avanti Polar Lipids, Inc. (Alabaster, AL, USA): 17:0- LPC, 18:1-LPC, 13:0/13:0- PC, 16:0/16:0-PC, 18:0p/18:1-PC, 17:1-lysophosphatidylethanolamine (LPE), 18:0-LPE, 12:0/12:0-phosphatidylethanolamine (PE), 14:0/14:0-PE, 17:0/17:0-PE, 17:1-lysophosphatidylglycerol (LPG), 14:0-LPG, 18:0-LPG, 12:0/12:0-phosphatidylglycerol (PG), 14:0/14:0-PG, 15:0/15:0-PG, 17:1-lysophosphatidylinositol (LPI), 17:0/20:4-phosphatidylinositol (PI), 16:0/18:2-PI, 17:0-lysophosphatidic acid (LPA), 17:0/17:0-phosphatidic acid (PA), d18:1/17:0-sphingomyelin (SM), d18:1/16:0-SM, d18:1/18:0-SM, d18:1/17:0- Cer, d18:1/14:0-Cer, d18:1/17:0-monohexosylceramide (MHC), d18:1/12:0-MHC, d18:1/16:0-dihexosylceramide (DHC), 17:0/17:0-diacylglycerol (DG), 17:0/17:1/17:0-triacylglycerol (TG), and d18:1/24:0-sulfatide (ST). Standard lipids with odd numbered fatty acyl chains were added to lipid extracts as a mixture of internal standards for quantification. Chemicals, including $CHCl_3$, NH_4OH, and NH_4HCO_3, were purchased from Sigma-Aldrich (St. Louis, MO, USA). HPLC grade solvents (CH_3CN, CH_3OH, isopropanol, and MS grade water) and methyl-*tert*-butyl ether (MTBE) were purchased from J.T. Baker (Phillipsburg, NJ, USA). Fused silica capillaries (20, 75, 100, and 200 μm inner diameter and 360 μm outer diameter) for plumbing and preparing capillary columns were purchased from Polymicro Technology (Phoenix, AZ, USA).

2.2. Patients and plasma sampling

Plasma samples were collected from patients with CAD after obtaining informed consent according to the permission of the Institutional Review Board of the Severance Hospital (Seoul, Korea). The study was conducted in accordance with the current version of the Declaration of Helsinki. From 30 participants with CAD, 10 with ACS (referred to ACS) (age = 55.2 ± 5.5) and 10 with stable CAD without ACS (age = 57.3 ± 6.9) were selected by excluding patients not taking a statin. Demographic data for the plasma samples are listed in Table 1. All plasma samples were kept at −80 °C.

Table 1
Demographic data for CAD with ACS (ACS) and CAD without ACS (stable CAD).

Factor	CAD without ACS (stable CAD, n = 10)	CAD with ACS (ACS, n = 10)
Age (years)	57.3 ± 6.9	55.2 ± 5.5
Sex, n (%) male	4 (40%)	6 (60%)
TG (mg/dL)	116.3 ± 35.1	107.1 ± 37.9
Total-cholestetol (mg/dL)	160.4 ± 42.9	182.4 ± 40.6
HDL-cholesterol (mg/dL)	39.5 ± 5.97	46.1 ± 10.47
LDL-cholesterol (mg/dL)	93.8 ± 44.0	112.6 ± 37.4
Final efflux (%)	18.74 ± 4.94	18.86 ± 7.10
Hyperlipidemia, n(%)	3 (30%)	3 (30%)
Smoker, n(%)	4 (40%)	1 (10%)
Diabetes, n(%)	2 (20%)	4 (40%)
BMI (kg/m^2)	24.65 ± 2.53	24.94 ± 2.15

2.3. Separation of HDL and LDL

Prior to sorting the lipoproteins from plasma samples by size, albumin and immunoglobulin G (IgG) were depleted using a ProteoPrep® Immunoaffinity Albumin & IgG Depletion Kit from Sigma Aldrich. Semi-preparative scale AF4 was used to separate lipoproteins by size with a polyvinyl chloride channel spacer: 26.6 cm (length) × 250 μm (thickness) with a trapezoidal decrease in channel width from 4.4 to 0.4 cm (Wyatt Technology Europe GmbH, Dernbach, Germany). A regenerated cellulose membrane (MWCO 10 kDa) purchased from Millipore (Danvers, MA, USA) was placed at the accumulation wall. The carrier solution used for AF4 was 0.1 M PBS buffer prepared with deionized (> 18 MΩ) water and filtered using a 0.22 μm nitrocellulose membrane filter from EMD Millipore (Billerica, MA, USA) prior to use. The carrier solution was delivered to the channel using an SP930D HPLC pump from Young-Lin Instruments (Seoul, Korea) via a model 7125 loop injector from Rheodyne (Cotati, CA, USA). For each injection, 250 μL of depleted sample (equivalent to 50 μL of raw plasma) was injected. The flow rates were 3.6 and 0.4 mL/min for the crossflow and outflow rates, respectively. Eluting lipoproteins were monitored with a model UV730D UV detector from Young-Lin at wavelengths of 280 nm for lipoprotein standards and 600 nm for plasma samples stained with Sudan black B (SBB) as shown in Fig. 1. Plasma samples were stained with SBB to determine the collection periods of the HDL and LDL fractions.

2.4. Lipid extraction

Each lipoprotein fraction collected from the AF4 separation was concentrated, then mixed with 300 μL of CH_3OH. The tube containing the mixture was placed in an ice bath for 10 min, then 1000 μL of MTBE was added and the solution was vortexed for 1 h. Thereafter, 250 μL of MS-grade H_2O was added to the tube, then the tube was vortexed for 10 min and centrifuged for 10 min at 1000 × *g*. The upper organic layer was transferred to a separate tube, then 300 μL of CH_3OH was added to the remaining bottom layer. The mixture was sonicated for 2 min, then centrifuged for 10 min at 1000 × *g*. The upper layer was removed and mixed with the previously collected organic layer. The tube containing the final mixture was sealed with a 0.45 μm MilliWrap PTFE membrane from Millipore to avoid lipid evaporation while it was vacuum dried for 12 h. The dried lipids were weighed and reconstituted in CH_3OH:H_2O (9:1, v/v) at a concentration of 5 μg/μL for nLC-ESI-MS/MS analysis.

2.5. Lipid analysis by nUPLC-ESI-MS/MS

The lipid molecular structures from each lipoprotein fraction were identified using a Dionex Ultimate 3000 RSLCnano System with an

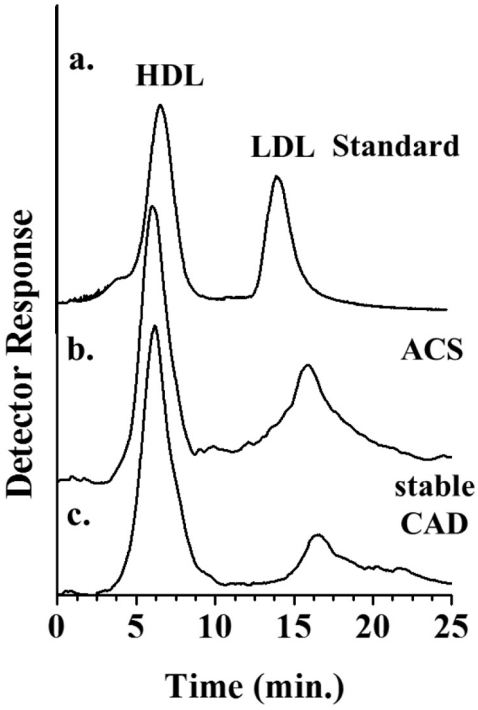

Fig. 1. Semi-preparative scale AF4 separation of a) a mixture of HDL and LDL standards, b) the plasma sample (stained with Sudan Black B) from patients with ACS and c) the plasma sample (stained with SBB) from patients with stable CAD obtained at $\dot{V}_{in}/\dot{V}_{out}$ = 4.0/0.4 (mL/min). Wave lengths of UV detection were 280 nm for a) and 600 nm for b) and c).

autosampler coupled with LTQ Velos ion trap mass spectrometer from Thermo Scientific (San Jose, CA, USA). The targeted quantitation of identified lipids were made using a nanoACQUITY UPLC system from Waters Co. (Milford, MA, USA) equipped with a TSQ Vantage triple-stage quadrupole MS system from Thermo Scientific. For both LC separations, the same analytical column was used by making a homemade capillary column with a fused silica capillary tube (100 μm I.D. and 360 μm O.D.). One end of capillary tube was pulled using a flame to form a needle-like tip, then a 0.5 cm portion of the column tip was filled with 3 μm Watchers® ODS-P C18 particles from Isu Industry Corp. (Seoul, Korea) as a self-assembled frit. Thereafter, the column was packed for 7 cm with 1.7 μm C18 particles (130 Å), which were unpacked from an XBridge® BEH C18 from Waters under nitrogen gas at 1000 psi. The connection of the analytical column for ESI is the same as described elsewhere [21,24].

The mobile phases of the binary gradient LC separations were (9:1, v/v) H_2O:CH_3CN for A and (2:2:6, v/v/v) CH_3OH:CH_3CN:IPA for B, which were added with 5 mM NH_4HCO_2 and 0.05% NH_4OH as a mixed ionization modifier for both the positive and negative ion modes. Each lipid extract (3 μL each, equivalent to 15 μg of lipids) was injected directly into the analytical column using 99% mobile phase A at 700 nL/min for 10 min. Thereafter, the pump flow rate was adjusted to 7.5 μL/min with the vent valve open so that only 300 nL/min of flow was allowed into the analytical column. The gradient elution for non-targeted lipid identification began by raising mobile phase B to 40% for 1 min, 80% for 10 min, 99% for 20 min, then maintained at 99% for 15 min. Thereafter, the mobile phase was decreased to 1% B and reconditioned for 15 min. The ESI voltage was 3.0 kV, the mass range for the precursor run was 400–1600 amu, and 40% of the normalized collision energy was applied for data-dependent CID analysis. Gradient elution for targeted lipid quantification began by ramping the mobile phase B to 50% for 1.5 min. Mobile phase B was then increased to 80% for 5 min, 100% for 10 min, and maintained for 5 min. Thereafter, the mobile phase was changed to 100% A and reconditioned for 15 min. Targeted quantification was based on the SRM of selected lipids by analysing a precursor ion and its class-specific product ions (Supplementary Table S1) in data-dependent CID experiments. SRM quantification was achieved at the switching ion mode (positive and negative ion modes alternatively) in a single run with a scan width of m/z 1.5, scan time of 0.001 s, and ESI voltage of 3 kV. The lipid classes LPG, PG, LPI, PI, LPA, and PA were analysed in the negative ion mode cycle, whereas the lipids classes LPC, PC, LPE, PE, PEp, DG, TG, Cer, SM, MHC, and DHC were analysed in the positive ion mode cycle. Collision energies were applied differently depending on the lipid class (Table S1). Lipids were quantified by calculating the corrected peak area, which is the ratio of the species peak area to that of the corresponding internal standard (IS) (1 pmol each injection), which was added to the lipid extract sample as a mixture of 15 standard lipids with odd-numbered fatty acyl chains.

3. Results and discussion

3.1. Size sorting of lipoproteins, lipid identification, and quantification

Fig. 1 shows the size separation of HDL and LDL from patient plasma samples utilizing AF4 in which separation takes place in an increasing order of particle diameters. Fig. 1 indicates that the LDL peaks for both groups of patients (ACS and stable CAD) were relatively broad compared to LDL standard peaks. In addition, the retention times of the patient samples were shifted to longer time scales than that of standard. These supported that the LDL particles of patients were larger and broader than typical standard LDL particles. It is likely that standard LDL particles were depleted with some associating proteins in their surface during purification process which may result in the decrease in sizes compared to LDL in plasma. However, retention of LDL from the ACS was not significantly different from that from stable CAD, indicating that there were no significant change in LDL sizes between the two groups. The broad distribution of LDL peak from both ACS and stable CAD may support that very low density lipoprotein (VLDL) and LDL were not completely separated from each other. Lipids extracted from each lipoprotein fraction (HDL and LDL including VLDL) were analysed by nUPLC-ESI-MS/MS to identify non-targeted molecular structures, then quantified using the SRM method. Base peak chromatograms (BPCs) of each lipid extract from patients with stable CAD and patients with ACS are compared in Supplementary Fig. S1 at the run conditions which demonstrated the separation of standard lipids in positive and negative ion modes shown in Supplementary Fig. S2. A total of 365 lipids from 13 classes were identified with their molecular structures from both the HDL and LDL fractions and the quantified results of individual species are compared between patients with ACS and stable CAD in each lipid class in Fig. 2. The results are expressed as corrected peak area, which is the peak area of a lipid species relative to the peak area of 1 pmol of each internal standard (IS) specific to the lipid class. A set of internal standards selected for each lipid class are listed in Supplementary Table S1 along with the types of precursor and product ions and the specific collision energy of the CID experiments for class specific SRM quantitation. Fig. 1 shows the difference in the total amount of lipids in 13 lipid classes in the HDL and LDL fractions between ACS and stable CAD and classifies the lipid classes according to a) no significant difference in total amount of each lipid class between ACS and stable CAD, b) moderate differences, and c) significant differences (> 2-fold). Lipids marked with acyl chain information in Fig. 2 are high abundance species in each class. A high abundance lipid is defined when the relative abundance of a lipid is > 100%/(total number of lipids within the class). The white bar marked “low” represents the summed amount of the remaining low abundance lipids. While the dominant lipid classes, such as PC and SM, were not significantly different in patients with ACS, the changes in the amount of PE, TG, and DG were distinct in both lipoprotein fractions (only LDL for DG). Fig. 1 also indicates the difference in lipid profiles between HDL and LDL at both individual lipid levels and lipid class. The quantified

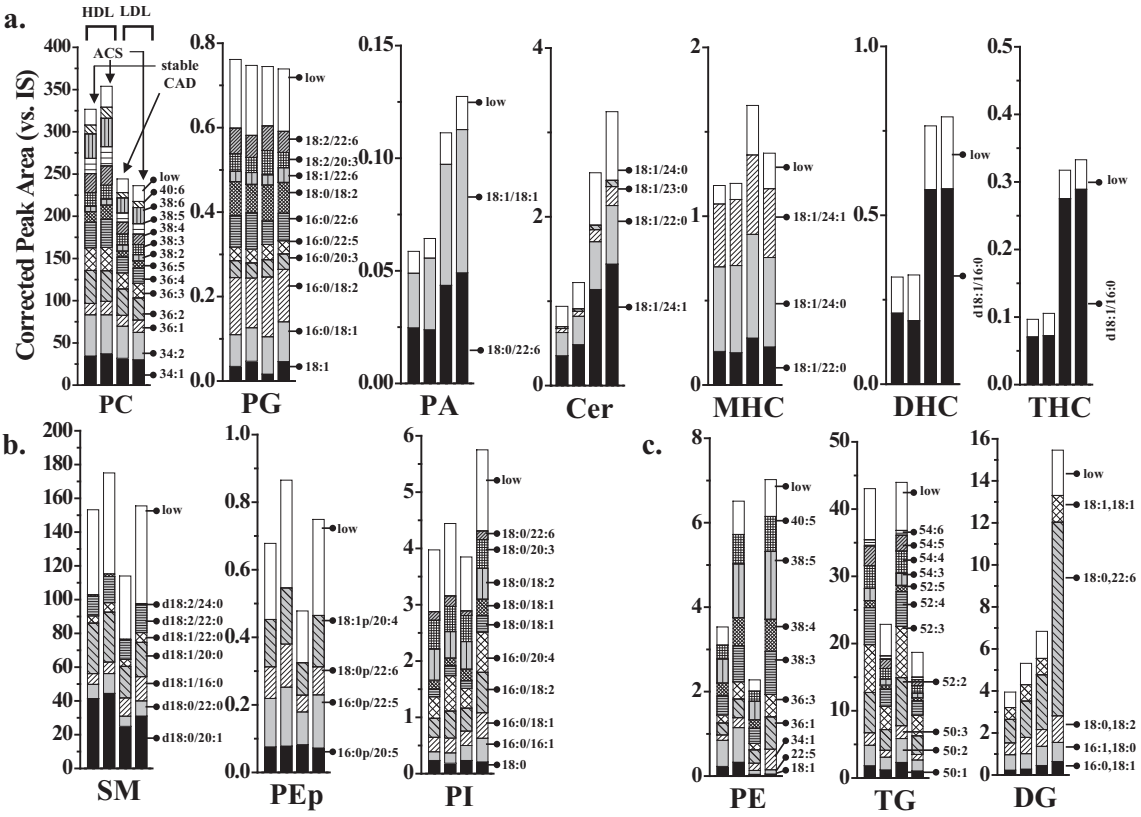

Fig. 2. Compositional distribution plotted as the corrected peak area (vs. I.S.) of differentially abundant lipid species in each lipid class. a) No significant difference between ACS and stable CAD groups, b) moderate difference, and c) significant difference (> 1.5 fold). The empty bar marked with "low" represents the summed amount of less-abundant lipids in each lipid class.

data of lipids with their corrected peak area values and the relative abundances are listed in Supplementary Table S2. Lipid species PC, PE, and TG were expressed with the total number of acyl chain lengths and double bonds because SRM quantification of these species can be done without differentiating geometrical isomers. The identified molecular structures of the isomers are tabulated in Supplementary Table S3.

3.2. Lipids showing significant changes in ACS

Differences in the amount of individual lipid species between ACS and stable CAD can be visualized in Fig. 3a with the volcano plots, $-\log_{10}$ (p-value) vs. $\log_2$ (fold ratio of ACS to stable CAD), of the 365 lipid species in the HDL and LDL fractions. Fig. 3a represents that the number of species with > 1.5-fold differences (vertical lines) is larger in LDL than in HDL. Principal component analysis (PCA) plots of lipids showing significant differences (> 1.5-fold, $p < 0.05$) between the ACS and stable CAD groups in Fig. 3b indicate a clear difference in lipid profiles between the ACS and stable CAD groups in both lipoprotein fractions. The heat map in Fig. 4 shows a clear difference in the individual amounts among selected lipids showing a > 1.5-fold difference and $p < 0.05$ in ACS compared to those in stable CAD. Individual lipid levels of PE, PEp, PI, and DG increased in the ACS group to a greater extent in LDL than in HDL, whereas TG decreased in both lipoproteins. Seven LPC species (14:0, 16:0. 16:1, 18:0, 18:3, 20:0, and 20:5) increased only in HDL in the ACS group, whereas the changes in LDL were negligible.

Changes in lipid composition were further examined by plotting pie charts in Fig. 5a. The pie charts represent the compositional variations in the high abundance PE species in both the HDL and LDL fractions. The relative occupancy of five high abundance PE species in the HDL fraction in Fig. 5a did not change between the two groups (ACS and stable CAD), whereas the total amount of PE in both fractions in ACS doubled. However, the relative abundance of the three PEs (38:4, 38:5, and 40:5) in LDL increased by approximately 50% and the total increase was 2.4-fold. Among these, 38:5-PE and 40:5-PE significantly increased in the ACS group by > 2-fold in both fractions ($p < 0.05$; Fig. 5b). High abundance lipid species with significant changes exhibited simultaneous increases or decreases in both HDL and LDL fractions. For instance, the levels of most PE species in Fig. 5b were elevated in LDL to a larger degree than in HDL. Overall, in both lipoprotein fractions, the high abundance PE levels greatly increased in the ACS group (> 2.5-fold). A previous study reported that the total plasma PE level in the unstable CAD group increased approximately 1.26-fold compared to that in the stable CAD group, whereas that of the stable CAD group increased to a greater extent (2.91 fold) compared to healthy controls [25]. Moreover, the four high abundance PEs (38:3, 38:4, 38:5, and 40:5) that increased (> 3-fold) in the ACS group of our study (Table 2) were reported to increase in the CAD patient group [25]. Among them, 38:4- and 38:5-PEs similarly increased to a lesser degree (~30%) in the unstable CAD group.

In the case of DG, a similar trend was observed in the HDL fraction between the ACS and stable CAD groups (Supplementary Fig. S3). However, some fluctuations in LDL were observed: the relative occupancy of (18:0, 22:6)-DG significantly increased to 59.6% from 38.1%, whereas those of the other four high abundance species decreased. Moreover, (18:0, 22:6)-DG among the four high abundance DG species increased > ~3.5 fold in the LDL of the ACS group.

Overall, the high abundance lipid species with more than a 1.5-fold difference and $p < 0.05$ in either HDL or LDL are summarized in Table 2. Among the lipid species with significant differences marked with asterisk (*), the fold ratios of 19 high abundance species are plotted in Fig. 6. Fig. 6a indicates that the two high abundance LPC species (16:0 and 18:0) significantly increased only in the HDL fraction, two PE species (38:5 and 40:5) significantly increased in both HDL

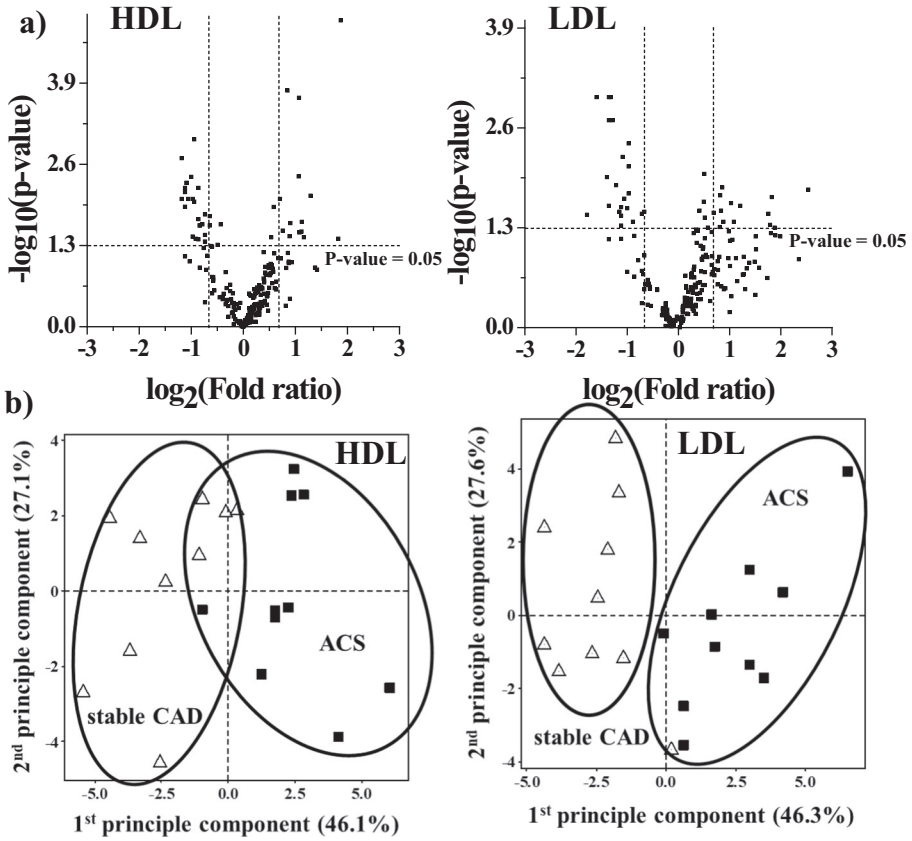

Fig. 3. a) Volcano plots plotted by $\log_{10}$ (p value) vs. $\log_2$ (fold ratio, ACS/stable CAD) of 365 lipids species of HDL and LDL fractions, and b) principle component analysis (PCA) plots representing the differences between the groups ACS (n = 10) and stable CAD (n = 10) based on lipids showing significant difference (> 1.5-fold, $p < 0.05$) in each lipoprotein fraction.

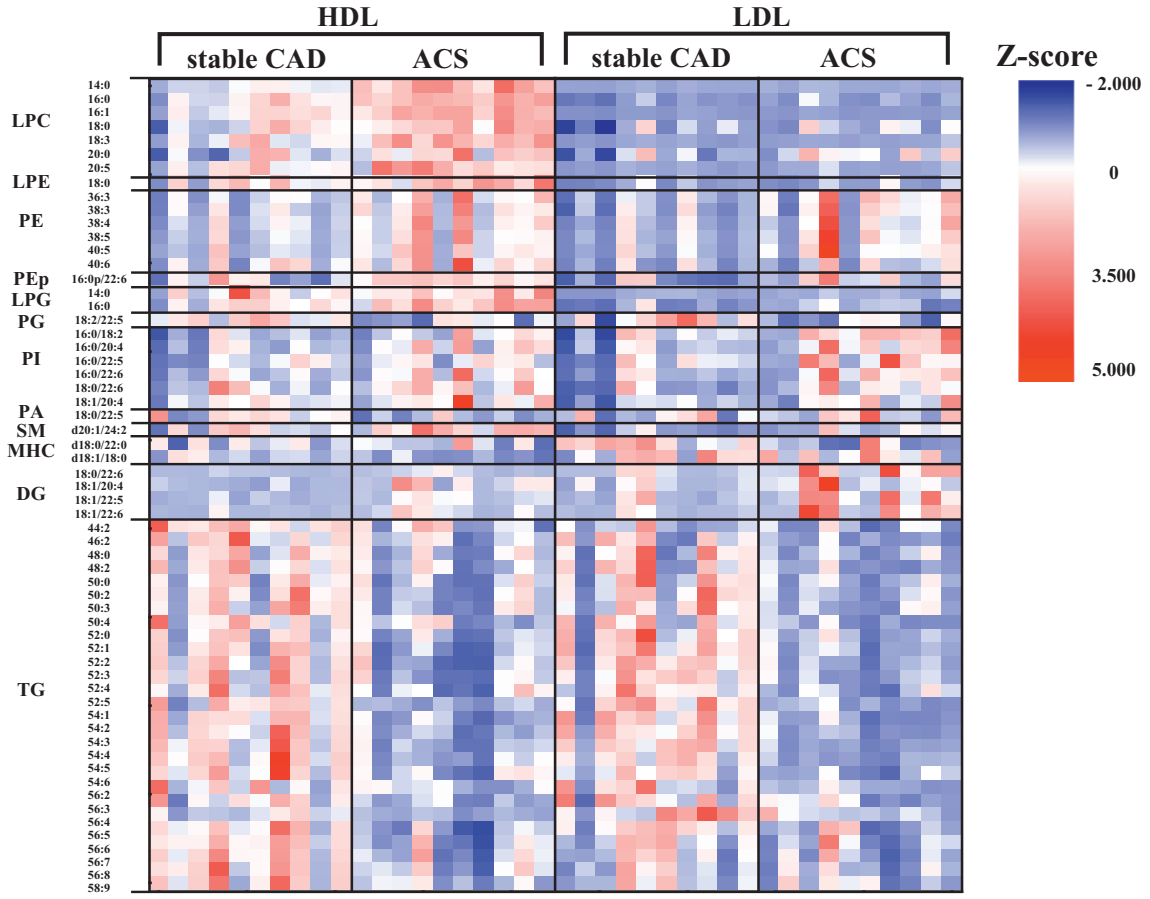

Fig. 4. Heat map of selected lipids (> 1.5-fold & $p < 0.05$) between ACS (n = 10) and stable CAD (n = 10) in HDL and LDL fractions.

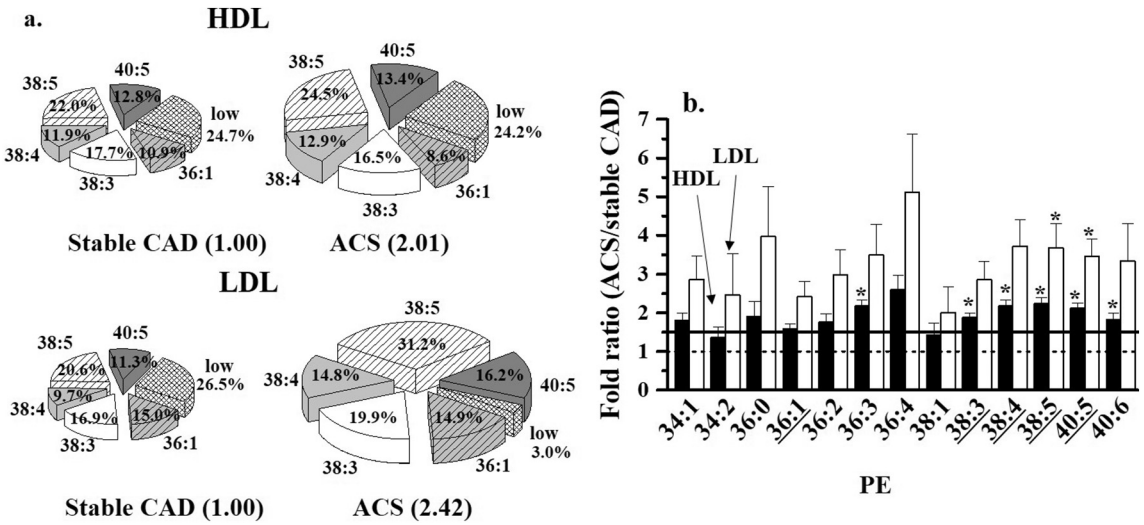

Fig. 5. a) Pie charts representing the compositional differences in PE species ("low" represents the summed amount of low abundance PE species) in HDL and LDL fractions, and b) fold ratio (ACS/stable CAD) of PE molecules showing > 1.5-fold: underlined species for high abundance species and * for the significant difference ($p < 0.05$).

(by > 2 fold) and LDL (by > 3.5 fold) in the ACS group, the other two PE species (38:3 and 38:4) significantly increased only in HDL, the three PI species (16:0/18:2, 16:0/20:4, and 18:0/22:6) and (18:0,22:6)-DG) increased only in the LDL of the ACS group, and most high abundance TGs decreased by nearly 2-fold in both lipoprotein fractions. LPC is a critical factor in the induction of the inflammatory pathways of atherosclerosis [26–29]. LPC levels were reported to increase in ACS patients and increase more in non-ST elevation myocardial infarction (NSTEMI) than in patients with stable angina [30]. In particular, LPC species with saturated or monounsaturated acyl chains increased inflammation and atherosclerosis, whereas LPC species with polyunsaturated fatty acids decreased the inflammatory response [31,32]. Seven LPC species that significantly increased in the ACS group of our study increased only in the HDL fraction. Among these species, 16:0-LPC and 18:0-LPC were high abundance species occupying 45.8% and 12.1% of all LPCs, respectively, indicating that dominant saturated LPCs were closely associated with the development of ACS in CAD patients.

Fig. 6b shows that total TG levels significantly decreased in the ACS group for both the HDL and LDL fractions compared to those in the stable CAD group, whereas there were no significant differences in the average TG levels of the whole blood measured by clinical analysis between the two groups in Table 1. A study also reported no significant differences in TG levels between patients with ACS and those with stable CAD [33]. Increases in DG levels can be explained by the decreased TG levels. In this study, the total DG level in the LDL of the ACS group increased approximately 2.3-fold (Fig. S3), which was attributed to the large increase in high abundance DG species with acyl chain structures: (18:0, 22:6)-, (18:0,18:2)-, and (18:1,18:1)-DG. This supported that the acyl chains from the TG species containing the same

Table 2
List of high abundance lipid species with significant difference (> 1.5-fold & $p < 0.05$) between the two CAD patients group (stable CAD and ACS) for HDL and LDL fractions obtained by nUPLC–ESI–MS/MS. Species marked with bold represent changes > 1.5-fold, * for $p < 0.05$, and ** for $p < 0.01$. "abun" represents the relative abundance of species in each lipid class.

Class	Molecular species	*m/z*	HDL		LDL	
			ACS/stable CAD	abun.(%)	ACS/stable CAD	abun.(%)
LPC	16:0	496.5	**1.80 ± 0.06****	45.75	1.40 ± 0.12	50.03
	18:0	524.5	**1.50 ± 0.03****	12.06	1.28 ± 0.04	29.09
PE	38:3	768.5	**1.87 ± 0.14***	17.76	**2.85 ± 0.50**	16.83
	38:4	766.5	**2.17 ± 0.18***	11.95	**3.72 ± 0.71**	9.68
	38:5	764.5	**2.24 ± 0.17***	21.78	**3.68 ± 0.64***	20.42
	40:5	792.5	**2.11 ± 0.17***	12.70	**3.46 ± 0.47***	11.55
PI	16:0/18:2	833.5	1.42 ± 0.09	9.93	**1.76 ± 0.20***	11.87
	16:0/20:4	857.5	**1.65 ± 0.12**	11.33	**2.04 ± 0.19***	10.45
	18:0/22:6	909.5	1.23 ± 0.12	4.46	**1.81 ± 0.23***	2.83
DG	18:0,22:6	686.5	**1.55 ± 0.23**	28.39	**3.54 ± 0.72***	34.85
TG	50:2	848.5	**0.62 ± 0.05**	7.03	**0.46 ± 0.04***	8.06
	50:3	846.5	**0.55 ± 0.04***	4.31	**0.43 ± 0.03***	4.27
	52:2	876.5	**0.51 ± 0.04****	14.64	**0.39 ± 0.03****	16.89
	52:3	874.5	**0.48 ± 0.03****	16.92	**0.40 ± 0.03****	17.87
	52:4	872.5	**0.46 ± 0.03***	12.47	**0.41 ± 0.04****	12.03
	52:5	870.5	**0.59 ± 0.05**	2.36	**0.50 ± 0.04***	2.12
	54:3	902.5	**0.50 ± 0.05****	4.02	**0.38 ± 0.03****	4.01
	54:4	900.5	**0.47 ± 0.05****	7.91	**0.34 ± 0.04****	7.11
	54:5	898.5	**0.46 ± 0.04****	6.70	**0.38 ± 0.04****	5.24

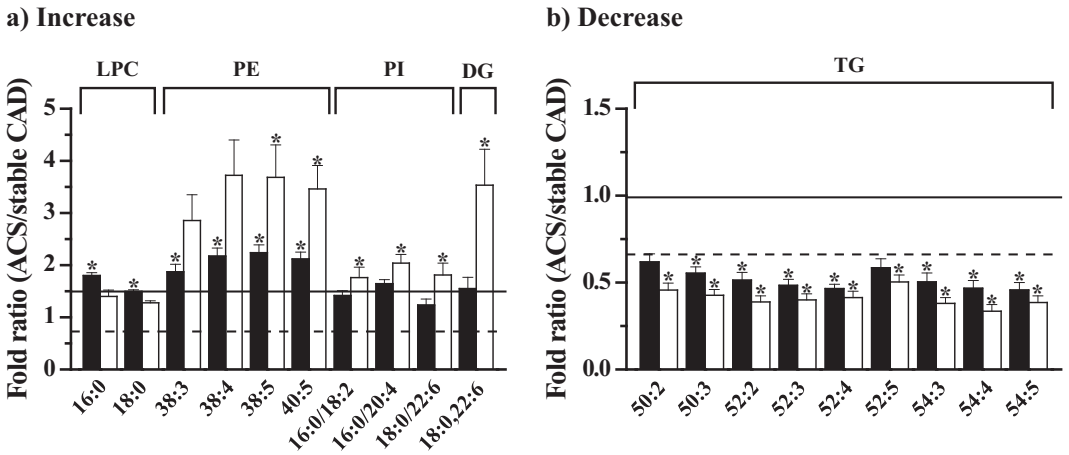

Fig. 6. Plots of fold ratio (ACS/stable CAD) of high abundance lipid species. a) increases and b) decreases > 1.5-fold with $p < 0.05$ (marked with *).

combination of two acyl chains could be dissociated. For instance, 54:6-, 54:7-, 56:7-, and 56:8-TG contain the two acyl chains of (18:0, 22:6), seven TGs have (18:0,18:2), and 11 TG species contain (18:1,18:1).

4. Conclusions

Lipidomic comparison between patients with ACS and those with stable CAD demonstrated the characteristic differences in their increase or decrease patterns in both the HDL and LDL fractions. Whereas levels of high abundance PEs and TGs in the ACS group increased and decreased, respectively, in both lipoprotein fractions, high abundance LPCs increased only in the HDL fraction. LPC species with saturated acyl chains increased in the ACS patients to a greater extent in HDL than in LDL, which suggested that saturated LPC species may be associated with the progression of ACS. The present study demonstrated that the plasma lipid profiles of patients with ACS compared to those in patients with stable CAD can be comprehensively analysed according to the types of lipoproteins by employing AF4 to sort lipoproteins by size prior to lipid analysis. Lipid species with significant differences in the ACS group can be used to understand the pathogenesis of ACS at the lipoprotein level and can be the basis of high speed screening of a large number of patient samples to develop potential lipid markers for the early prediction of ACS.

Acknowledgements

This study was supported by the grants NRF-2018R1A2A1A005019794 and NRF- 2015R1A2A1A01004677 from the National Research Foundation of Korea.

Conflict of interest

All authors declare no conflict of interest related to this work.

Appendix A. Supplementary data

Supplementary data to this article can be found online at https://doi.org/10.1016/j.jchromb.2018.09.016.

References

[1] C.K. Glass, J.L. Witztum, Atherosclerosis. The road ahead, Cell 104 (2001) 503–516.
[2] P. Libby, P. Theroux, Pathophysiology of coronary artery disease, Circulation 111 (2005) 3481–3488.
[3] R. Meshkani, K. Adeli, Hepatic insulin resistance, metabolic syndrome and cardiovascular disease, Clin. Biochem. 42 (2009) 1331–1346.
[4] L. Slama, C. Le Camus, L. Serfaty, G. Pialoux, J. Capeau, S. Gharakhanian, Metabolic disorders and chronic viral disease: the case of HIV and HCV, Diabete Metab. 35 (2009) 1–11.
[5] J.M. Cheng, M. Suoniemi, I. Kardys, T. Vihervaara, S.P. de Boer, K.M. Akkerhuis, M. Sysi-Aho, K. Ekroos, H.M. Garcia-Garcia, R.M. Oemrawsingh, E. Regar, W. Koenig, P.W. Serruys, R.J. van Geuns, E. Boersma, R. Laaksonen, Plasma concentrations of molecular lipid species in relation to coronary plaque characteristics and cardiovascular outcome: results of the ATHEROREMO-IVUS study, Atherosclerosis 243 (2015) 560–566.
[6] Z.H. Alshehry, P.A. Mundra, C.K. Barlow, N.A. Mellett, G. Wong, M.J. McConville, J. Simes, A.M. Tonkin, D.R. Sullivan, E.H. Barnes, P.J. Nestel, B.A. Kingwell, M. Marre, B. Neal, N.R. Poulter, A. Rodgers, B. Williams, S. Zoungas, G.S. Hillis, J. Chalmers, M. Woodward, P.J. Meikle, Plasma lipidomic profiles improve on traditional risk factors for the prediction of cardiovascular events in type 2 diabetes mellitus, Circulation 134 (2016) 1637–1650.
[7] C. Syme, S. Czajkowski, J. Shin, M. Abrahamowicz, G. Leonard, M. Perron, L. Richer, S. Veillette, D. Gaudet, L. Strug, Y. Wang, H. Xu, G. Taylor, T. Paus, S. Bennett, Z. Pausova, Glycerophosphocholine metabolites and cardiovascular disease risk factors in adolescents: a cohort study, Circulation 134 (2016) 1629–1636.
[8] M. Hilvo, H. Simolin, J. Metso, M. Ruuth, K. Oorni, M. Jauhiainen, R. Laaksonen, A. Baruch, PCSK9 inhibition alters the lipidome of plasma and lipoprotein fractions, Atherosclerosis 269 (2018) 159–165.
[9] P.J. Meikle, G. Wong, C.K. Barlow, B.A. Kingwell, Lipidomics: potential role in risk prediction and therapeutic monitoring for diabetes and cardiovascular disease, Pharmacol. Ther. 143 (2014) 12–23.
[10] K. Paapstel, J. Kals, J. Eha, K. Tootsi, A. Ottas, A. Piir, M. Jakobson, J. Lieberg, M. Zilmer, Inverse relations of serum phosphatidylcholines and lysophosphatidylcholines with vascular damage and heart rate in patients with atherosclerosis, Nutr. Metab. Cardiovasc. Dis. 28 (2018) 44–52.
[11] S. Heimerl, A. Boettcher, H. Kaul, G. Liebisch, Lipid profiling of lipoprotein X: implications for dyslipidemia in cholestasis, Biochim. Biophys. Acta 1861 ((2016) 681–687.
[12] C. Garcia, N. Montee, J. Faccini, J. Series, O. Meilhac, A.V. Cantero, P. Le Faouder, M. Elbaz, B. Payrastre, C. Vindis, Acute coronary syndrome remodels the antiplatelet aggregation properties of HDL particle subclasses, J. Thromb. Haemost. 16 (2018) 933–945.
[13] J.Y. Lee, S.K. Byeon, M.H. Moon, Profiling of oxidized phospholipids in lipoproteins from patients with coronary artery disease by hollow fiber flow field-flow fractionation and nanoflow liquid chromatography-tandem mass spectrometry, Anal. Chem. 87 (2015) 1266–1273.
[14] J. Godzien, M. Ciborowski, E.G. Armitage, I. Jorge, E. Camafeita, E. Burillo, J.L. Martin-Ventura, F.J. Ruperez, J. Vazquez, C. Barbas, A single in-vial dual extraction strategy for the simultaneous lipidomics and proteomics analysis of HDL and LDL fractions, J. Proteome Res. 15 (2016) 1762–1775.
[15] S. Ehara, M. Ueda, T. Naruko, K. Haze, A. Itoh, M. Otsuka, R. Komatsu, T. Matsuo, H. Itabe, T. Takano, Y. Tsukamoto, M. Yoshiyama, K. Takeuchi, J. Yoshikawa, A.E. Becker, Elevated levels of oxidized low density lipoprotein show a positive relationship with the severity of acute coronary syndromes, Circulation 103 (2001) 1955–1960.
[16] M. Navab, S.Y. Hama, S.T. Reddy, C.J. Ng, B.J. Van Lenten, H. Laks, A.M. Fogelman, Oxidized lipids as mediators of coronary heart disease, Curr. Opin. Lipidol. 13 (2002) 363–372.
[17] A. Litzen, J.K. Walter, H. Krischollek, K.G. Wahlund, Separation and quantitation of monoclonal antibody aggregates by asymmetrical flow field-flow fractionation and comparison to gel permeation chromatography, Anal. Biochem. 212 (1993) 469–480.
[18] P. Reschiglian, M.H. Moon, Flow field-flow fractionation: a pre-analytical method for proteomics, J. Proteome 71 (2008) 265–276.
[19] P. Reschiglian, A. Zattoni, B. Roda, S. Casolari, M.H. Moon, J. Lee, J. Jung, K. Rodmalm, G. Cenacchi, Bacteria sorting by field-flow fractionation. Application to whole-cell *Escherichia coli* vaccine strains, Anal. Chem. 74 (2002) 4895–4904.

[20] J.S. Yang, J.Y. Lee, M.H. Moon, High speed size sorting of subcellular organelles by flow field-flow fractionation, Anal. Chem. 87 (2015) 6342–6348.
[21] J.S. Yang, J.C. Lee, S.K. Byeon, K.H. Rha, M.H. Moon, Size dependent lipidomic analysis of urinary exosomes from patients with prostate cancer by flow field-flow fractionation and nanoflow liquid chromatography-tandem mass spectrometry, Anal. Chem. 89 (2017) 2488–2496.
[22] J.C. Giddings, Field flow fractionation. A versatile method for the characterization of macromolecular and particulate materials, Anal. Chem. 53 (1981) 1170A–1178A.
[23] M. Nilsson, S. Birnbaum, K.G. Wahlund, Determination of relative amounts of ribosome and subunits in *Escherichia coli* using asymmetrical flow field-flow fractionation, J. Biochem. Biophys. Methods 33 (1996) 9–23.
[24] J.C. Lee, S.K. Byeon, M.H. Moon, Relative quantification of phospholipids based on isotope-labeled methylation by nanoflow ultrahigh performance liquid chromatography-tandem mass spectrometry: enhancement in cardiolipin profiling, Anal. Chem. 89 (2017) 4969–4977.
[25] P.J. Meikle, G. Wong, D. Tsorotes, C.K. Barlow, J.M. Weir, M.J. Christopher, G.L. MacIntosh, B. Goudey, L. Stern, A. Kowalczyk, I. Haviv, A.J. White, A.M. Dart, S.J. Duffy, G.L. Jennings, B.A. Kingwell, Plasma lipidomic analysis of stable and unstable coronary artery disease, Arterioscler. Thromb. Vasc. Biol. 31 (2011) 2723–2732.
[26] L. Chen, B. Liang, D.E. Froese, S. Liu, J.T. Wong, K. Tran, G.M. Hatch, D. Mymin, E.A. Kroeger, R.Y. Man, P.C. Choy, Oxidative modification of low density lipoprotein in normal and hyperlipidemic patients: effect of lysophosphatidylcholine composition on vascular relaxation, J. Lipid Res. 38 (1997) 546–553.
[27] R. Wu, Y.H. Huang, L.S. Elinder, J. Frostegard, Lysophosphatidylcholine is involved in the antigenicity of oxidized LDL, Arterioscler. Thromb. Vasc. Biol. 18 (1998) 626–630.
[28] G. Schmitz, K. Ruebsaamen, Metabolism and atherogenic disease association of lysophosphatidylcholine, Atherosclerosis 208 (2010) 10–18.
[29] O.A. Akerele, S.K. Cheema, Fatty acyl composition of lysophosphatidylcholine is important in atherosclerosis, Med. Hypotheses 85 (2015) 754–760.
[30] M. Calderon-Santiago, F. Priego-Capote, J.G. Galache-Osuna, M.D. Luque De Castro, Analysis of serum phospholipid profiles by liquid chromatography-tandem mass spectrometry in high resolution mode for evaluation of atherosclerotic patients, J. Chromatogr. A 1371 (2014) 154–162.
[31] N. Aiyar, J. Disa, Z. Ao, H. Ju, S. Nerurkar, R.N. Willette, C.H. Macphee, D.G. Johns, S.A. Douglas, Lysophosphatidylcholine induces inflammatory activation of human coronary artery smooth muscle cells, Mol. Cell. Biochem. 295 (2007) 113–120.
[32] N.D. Hung, D.E. Sok, M.R. Kim, Prevention of 1-palmitoyl lysophosphatidylcholine-induced inflammation by polyunsaturated acyl lysophosphatidylcholine, Inflamm. Res. 61 (2012) 473–483.
[33] A. Vonbank, C.H. Saely, P. Rein, H. Drexel, Lipid parameters in patients with acute coronary syndromes versus stable coronary artery disease, Eur. J. Clin. Investig. 45 (2015) 1092–1097.